The two-fold singularity of nonsmooth flows: leading order dynamics in n-dimensions

Alessandro Colombo* & Mike R. Jeffrey†

July 23, 2013

Abstract

A discontinuity in a system of ordinary differential equations can create a flow that slides along the discontinuity locus. Prior to sliding, the flow may have collapsed onto the discontinuity, making the reverse flow non-unique, as happens when dry-friction causes objects to stick. Alternatively, a flow may slide along the discontinuity before escaping it at some indeterminable time, implying non-uniqueness in forward time. At a two-fold singularity these two behaviours are brought together, so that a single point may have multiple possible futures as well as histories. Two-folds are a generic consequence of discontinuities in three or more dimensions, and play an important role in both local and global dynamics. Despite this, until now nothing was known about two-fold singularities in systems of more than 3 dimensions. Here, the normal form of the two-fold is extended to higher dimensions, where we show that much of its lower dimensional dynamics survives.

1 Introduction

Dynamical systems that suffer sharp systemic changes can be modelled using nonsmooth differential equations. Examples include the directionality of Coulomb's friction, and various kinds of switching in electronic circuits, in models of biological growth, or in predator-prey interaction; for recent reviews see [9, 21] and references therein. Switching gives rise to a flow that is smooth everywhere, except on some hypersurface where its time derivative is discontinuous.

*DEIB, Politecnico di Milano, Milan, Italy, email:alessandro.colombo@polimi.it

†Department of Engineering Mathematics, University of Bristol, UK, email: mike.jeffrey@bristol.ac.uk

A discontinuity can have a dramatic effect on the properties of the flow. While a smooth flow is topologically equivalent to a constant flow in a region where it is non-stationary, the same is not always true at a discontinuity, and this leads to richer local dynamics. As a result, while dynamics in smooth systems tends to be organised by stationary points, as in figure 1(i), dynamics in piecewise-smooth systems also depends heavily on tangencies between a flow and its discontinuity hypersurface, as in figure 1(ii)-(iii). At such tangencies the flow is typically non-stationary.

Figure 1: Simple singularities: (i) a stationary point, (ii)-(iii) tangencies between a flow and a line of discontinuity (dashed), known as (ii) a visible fold or (iii) an invisible fold.

A local analysis of tangencies can reveal much about the generic dynamics and bifurcations associated with discontinuities. The nearby dynamics can be characterized by a canonical set of equations – a normal form – possessing the least number of terms necessary for a given tangency to exist. These have been given for various types of tangency in low dimensions, see for example [17, 19, 20]. In some cases they can be trivially extended to arbitrary dimensions by rectifying the flow in the additional dimensions, but in many cases such an extension is not at all trivial.

The key section of this paper concerns the two-fold – a tangency whose rich local dynamics makes its generalization to higher dimensions particularly challenging, whose structural stability has long been in question, and for which the transformations to obtain low dimensional normal forms have been lacking.

The most basic of the tangencies in a piecewise-smooth flow is a *fold*, where the flow curves parabolically (is *folded*) with respect to the discontinuity hypersurface. Because of the discontinuity the flow can be tangent to the hypersurface from one side but transverse to it from the other (figure 1(ii)-(iii)). At a *two-fold* singularity (or simply a two-fold), the flow is tangent to the hypersurface on *both* sides, as depicted in figure 2. The two-fold comes in several types, each with their own generic dynamics. This singularity arose in the early literature on nonsmooth differential equations [1, 13, 18], and Teixeira [19] highlighted its importance if a substantial theory of nonsmooth dynamics was to be achieved (and a particularly challenging case of two-fold is now known as the *Teixeira singularity*). The counterintuitivity of its flow has since led to various misconceptions, particularly regarding its

structural stability and attractivity, which have been largely resolved in low dimensions by an explicit focus on dynamics [7, 15]. What remains unclear is whether any of the known dynamics is observed in higher dimensions. This will be addressed here by deriving a normal form for the two-fold in a general number of dimensions, consistent with those given in previous literature when reduced to three dimensions. This local analysis is a first step towards the greater problem of studying the role that two-fold singularities play in global dynamics in higher dimensions.

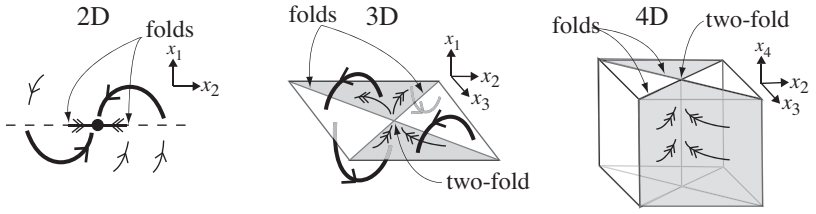

Figure 2: A discontinuity hypersurface has codimension one, folds have codimension two, and the two-fold has codimension three. As a consequence, the two-fold singularity generically arises in systems with at least three dimensions. (i) In two dimensions, pairs of folds do not typically coincide. (ii) In three dimensions, folds form curves on the discontinuity surface, which can intersect at a two-fold. (iii) In four dimensions the folds are surfaces and their intersection curve is a two-fold, here we depict the three dimensional space of the discontinuity surface. Double arrows indicate motion sliding along the discontinuity surface (in shaded regions).

As new dynamical phenomena are associated with this singularity, its potential implications in applications become more intriguing. A key feature of the two-fold is that the flow can be non-unique at the singularity, both in backward and forward time. Non-uniqueness is well understood to arise in nonsmooth systems because of *sliding*, whereby the flow becomes constrained to evolve along the discontinuity hypersurface. Non-uniqueness in backward time due to sliding has proven consistent with switching phenomena observed in physical, biological, stochastic, and engineering systems; see for example [9, 21]. The physical implications of non-uniqueness in forward time are only beginning to emerge, but are known to lead to a notion of discontinuity-induced explosions [5, 6, 14, 16], a non-deterministic form of chaos [7], and a nonsmooth analogue of canards related to the loss of hyperbolicity of critical manifolds in singularly perturbed systems [8].

In sections 2-3, the standard description of dynamics at a discontinuity is summarized (using a slightly unconventional but effective notation). The two-fold is defined and its normal form is given in section 4, extending previous results to n-dimensions. In section 5 we collect elements of the known classification of two-folds which, through Theorem 2 in section 4,

extend immediately into higher dimensions. Extensions to the theory are suggested in section 6, and the geometry underlying an important quantity in the classification is given in Appendix A.

2 Dynamics at a discontinuity

Throughout the paper we use the following notation (introduced in [12]). We are concerned only with small regions in which the discontinuity surface is smooth, so we define it as the zero set of a smooth function $\sigma(\mathbf{x}) : \mathbb{R}^n \to \mathbb{R}$. We use the symbol ∂_{t^+} to denote the Lie derivative operator along the flow in the region $\sigma(\mathbf{x}) > 0$, which we call the *upper* flow, and use ∂_{t^-} to denote the Lie operator along the flow in the region $\sigma(\mathbf{x}) < 0$, which we call the *lower* flow. For brevity we write $\partial_{t^\pm}$ in formulae that hold for both ∂_{t^+} and ∂_{t^-}, while the symbols $\partial_{t^+}\partial_{t^-}$ and $\partial^2_{t^+} = \partial_{t^+}\partial_{t^+}$, for example, denote second derivatives. The gradient operator is denoted by $\partial_{\mathbf{x}}$.

Let us combine ∂_{t^+} and ∂_{t^-} into a single time derivative operator,

$$\partial_{t^\lambda} := \lambda\partial_{t^+} + (1-\lambda)\partial_{t^-}, \tag{1}$$

and write:

Definition 1. *The time derivative operator along a piecewise smooth flow is given by*

$$\frac{d}{dt} := \{\, \partial_{t^\lambda} : \lambda \in \Lambda(\mathbf{x}) \,\}, \qquad \Lambda(\mathbf{x}) := \begin{cases} 1 & \text{if} \quad \sigma(\mathbf{x}) > 0, \\ [0,1] & \text{if} \quad \sigma(\mathbf{x}) = 0, \\ 0 & \text{if} \quad \sigma(\mathbf{x}) < 0. \end{cases} \tag{2}$$

This operator generates a piecewise smooth flow whose vector field $d\mathbf{x}/dt$ is equal to $\partial_{t^+}\mathbf{x}$ for $\sigma > 0$, $\partial_{t^-}\mathbf{x}$ for $\sigma < 0$, and is set-valued where $\sigma = 0$. Following the definition proposed by Filippov [13], we can say:

Definition 2. *A trajectory in the piecewise-smooth system generated by (2) is any absolutely continuous function $\mathbf{x}(t) : \mathbb{R} \to \mathbb{R}^n$ whose derivative belongs to $\frac{d}{dt}\mathbf{x}(t)$ almost everywhere.*

Although the flow generated by (2) is typically set-valued at $\sigma = 0$, only certain forms of dynamics are possible under definition 2. If

$$(\partial_{t^+}\sigma(\mathbf{x}))(\partial_{t^-}\sigma(\mathbf{x})) > 0 \qquad \text{on} \quad \sigma(\mathbf{x}) = 0, \tag{3}$$

then all vectors in $\frac{d}{dt}\mathbf{x}$ lie transverse to $\sigma = 0$, and the flow is said to *cross* the discontinuity surface (see figure 3, unshaded region). When a trajectory

$\mathbf{x}(t)$ crosses $\sigma = 0$, its tangent vector switches from $\partial_{t^+}\mathbf{x}(t)$ in $\sigma > 0$ to $\partial_{t^-}\mathbf{x}(t)$ in $\sigma < 0$, or vice versa. If instead

$$(\partial_{t^+}\sigma(\mathbf{x}))(\partial_{t^-}\sigma(\mathbf{x})) < 0 \qquad \text{on} \quad \sigma(\mathbf{x}) = 0, \tag{4}$$

then the set $\frac{d}{dt}\mathbf{x}$ contains a vector, $\partial_{t^s}\mathbf{x}$, lying in the tangent space to the discontinuity surface $\sigma = 0$, and given by

$$\partial_{t^s}\mathbf{x} := \frac{\partial_{t^-}\sigma}{(\partial_{t^-} - \partial_{t^+})\sigma}\partial_{t^+}\mathbf{x} + \left(1 - \frac{\partial_{t^-}\sigma}{(\partial_{t^-} - \partial_{t^+})\sigma}\right)\partial_{t^-}\mathbf{x}\,. \tag{5}$$

The system then admits trajectories that slide along the discontinuity surface (see figure 3, shaded regions), and the corresponding flow is called a *sliding flow*. This happens in regions that attract the surrounding flow (when $\partial_{t^+}\sigma < 0 < \partial_{t^-}\sigma$), called *sliding regions*, where a trajectory $\mathbf{x}(t)$ may have tangent vector $\partial_{t^+}\mathbf{x}(t)$ in $\sigma > 0$ or $\partial_{t^-}\mathbf{x}(t)$ in $\sigma < 0$, switching to $\partial_{t^s}\mathbf{x}(t)$ if the trajectory reaches $\sigma = 0$. Sliding also occurs in regions that repel the surrounding flow (when $\partial_{t^-}\sigma < 0 < \partial_{t^+}\sigma$), called *escaping regions*, where a trajectory $\mathbf{x}(t)$ lying in $\sigma = 0$ may have tangent vector $\partial_{t^s}\mathbf{x}(t)$, switching to $\partial_{t^+}\mathbf{x}(t)$ or $\partial_{t^-}\mathbf{x}(t)$ at any time and thus departing into $\sigma > 0$ in $\sigma < 0$. Since $\partial_{t^\pm}\sigma \neq 0$, the flow takes only a finite amount of time to reach or depart the discontinuity surface at a sliding or escaping region.

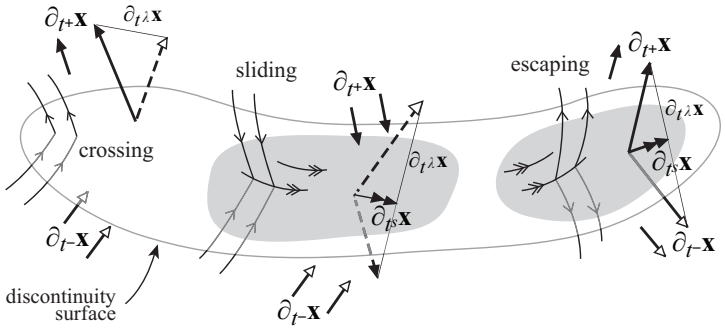

Figure 3: Dynamics at the discontinuity surface. A convex set $\frac{d}{dt}\mathbf{x}$ made up of vectors $\partial_{t^\lambda}\mathbf{x} = \lambda\partial_{t^+}\mathbf{x} + (1-\lambda)\partial_{t^-}\mathbf{x}$ interpolates between the vectors $\partial_{t^+}\mathbf{x}$ (black arrowheads) of the flow above, and $\partial_{t^-}\mathbf{x}$ (white arrowheads) of the flow below, the discontinuity surface. Some trajectories in the flow are shown. If $\partial_{t^\lambda}\mathbf{x}$ is transverse to the discontinuity surface, the flow crosses (unshaded). If the set contains a vector $\partial_{t^s}\mathbf{x}$ tangent to the surface, the flow slides in that direction, in sliding or escaping regions (shaded).

The flow is tangent to the discontinuity when the normal components of the velocity vectors, given by $\partial_{t^\pm}\sigma$, vanish. Points of tangency constitute singularities of the flow with respect to its discontinuity, the most fundamental of which are explored in this paper.

In the next section we describe the simplest of these tangencies, the fold, in preparation for our main topic, the two-fold, which then forms the remainder of the paper.

3 Folds

Definition 3. *A point* $\hat{\mathbf{x}}$ *where*

$$\sigma(\hat{\mathbf{x}}) = \partial_{t^+}\sigma(\hat{\mathbf{x}}) = 0, \qquad \partial_{t^-}\sigma(\hat{\mathbf{x}}) \neq 0,\ \partial^2_{t^+}\sigma(\hat{\mathbf{x}}) \neq 0 \tag{6}$$

defines a fold with respect to the upper flow, and a point $\hat{\mathbf{x}}$ *where*

$$\sigma(\hat{\mathbf{x}}) = \partial_{t^-}\sigma(\hat{\mathbf{x}}) = 0, \qquad \partial_{t^+}\sigma(\hat{\mathbf{x}}) \neq 0,\ \partial^2_{t^-}\sigma(\hat{\mathbf{x}}) \neq 0. \tag{7}$$

defines a fold with respect to the lower flow.

Folds are points of quadratic contact between the discontinuity surface and the flow from one side of $\sigma = 0$ or the other. The conditions in (6) or (7) imply that $\partial_{t^+}\sigma$ or $\partial_{t^-}\sigma$ change sign at the fold. As a result, recalling the conditions in (3) and (4), folds are typically boundaries between regions of crossing and sliding/escaping on the discontinuity surface, as shown in figure 4.

Theorem 1. *Let the point* $\hat{\mathbf{x}} = 0$ *be a fold on a discontinuity surface* $\sigma(\mathbf{x}) = 0$*. Then there exist coordinates* $\mathbf{x} = (x_1, x_2, ..., x_n)$ *in which the vector field is given by*

$$\left.\begin{array}{l} \frac{d}{dt}(x_1, x_2) = \left\{ \begin{array}{lll} \left(x_2,\ \operatorname{sgn}\left[\partial^2_{t^+}\sigma(0)\right] + \mathsf{O}\left(|\mathbf{x}|\right) \right) & \text{if} & x_1 > 0, \\ \left(\operatorname{sgn}\left[\partial_{t^-}\sigma(0)\right]\ ,\quad \mathsf{O}\left(|\mathbf{x}|\right) \right) & \text{if} & x_1 < 0, \end{array} \right. \\ \frac{d}{dt}x_i\ = \mathsf{O}\left(|\mathbf{x}|\right) \quad \text{for}\ \ i = 3, ..., n. \end{array}\right\} \tag{8}$$

Proof. Choose coordinates

$$x_1 = \alpha(\mathbf{x})\sigma(\mathbf{x})\,, \qquad x_2 = \gamma(\mathbf{x})\left(\beta(\mathbf{x})\sigma(\mathbf{x}) + \partial_{t^+}\sigma(\mathbf{x})\right), \tag{9}$$

in terms of functions

$$\gamma(\mathbf{x}) = \frac{1}{|\partial^2_{t^+}\sigma(\mathbf{x})|}\,, \quad (\alpha(\mathbf{x}), \beta(\mathbf{x})) = \left\{ \begin{array}{ll} \left(\gamma(\mathbf{x}),\ \frac{1}{\gamma}(\mathbf{x})\partial_{t^+}\gamma(\mathbf{x})\right) & \text{if}\ \ x_1 > 0\,, \\ \left(1,\ -\frac{\partial_{t^-}\partial_{t^+}\sigma(\mathbf{x})}{\partial_{t^-}\sigma(\mathbf{x})}\right) & \text{if}\ \ x_1 < 0\,. \end{array} \right. \tag{10}$$

The quantities $\alpha\sigma$ and $\beta\sigma$ are continuous (since $x_1 = 0$ coincides with $\sigma = 0$), hence the righthand sides in (9) are continuous but nondifferentiable at

$x_1 = 0$. The inequalities in (6) guarantee that the functions α, β, γ, are finite, and that α and γ are nonzero. Applying the operators $\partial_{t^\pm}$ from (2) gives

$$\tfrac{d}{dt}(x_1, x_2) = \begin{cases} \left(x_2 \ , \ \operatorname{sgn}[\partial^2_{t^+}\sigma(\mathbf{x})] + \mathbf{x}\cdot\boldsymbol{\varepsilon}^+(\mathbf{x}) \right) & \text{if} \quad x_1 > 0, \\ \left(\partial_{t^-}\sigma(\mathbf{x}) \ , \ \mathbf{x}\cdot\boldsymbol{\varepsilon}^-(\mathbf{x}) \right) & \text{if} \quad x_1 < 0, \end{cases} \tag{11}$$

where (omitting the argument $\mathbf{x}$)

$$\boldsymbol{\varepsilon}^+ = \left(\partial_{t^+}\left(\tfrac{\partial_{t^+}\gamma}{\gamma}\right) - \left(\tfrac{\partial_{t^+}\gamma}{\gamma}\right)^2, \ 2\tfrac{\partial_{t^+}\gamma}{\gamma}, \ 0, 0, ... \right) ,$$
$$\boldsymbol{\varepsilon}^- = \left(\ -\gamma\partial_{t^-}\left(\tfrac{\partial_{t^-}\partial_{t^+}\sigma}{\partial_{t^-}\sigma}\right) \quad , \ \tfrac{\partial_{t^-}\gamma}{\gamma} \ , \ 0, 0, ... \right).$$

We can rescale time by $t \mapsto t/\mu$ without changing the phase portrait of the flow, provided μ is strictly positive (this remains true if μ is only piecewise-smooth, see Appendix B). Let $\mu = 1$ for $x_1 > 0$ and let $\mu = |\partial_{t^-}\sigma|$ for $x_1 < 0$, giving

$$\tfrac{d}{dt}(x_1, x_2) = \begin{cases} \left(x_2, \ \operatorname{sgn}[\partial^2_{t^+}\sigma(\mathbf{x})] + \mathbf{x}\cdot\boldsymbol{\varepsilon}^+(\mathbf{x}) \right) & \text{if} \quad x_1 > 0, \\ \left(\operatorname{sgn}[\partial_{t^-}\sigma(\mathbf{x})], \ \mathbf{x}\cdot\boldsymbol{\varepsilon}^-(\mathbf{x})/|\partial_{t^-}\sigma(\mathbf{x})| \right) & \text{if} \quad x_1 < 0. \end{cases} \tag{12}$$

Taking a series expansion about $\hat{\mathbf{x}} = 0$ gives the first line of the theorem,

$$\tfrac{d}{dt}(x_1, x_2) = \begin{cases} \left(x_2, \ \operatorname{sgn}[\partial^2_{t^+}\sigma(0)] + \mathsf{O}\left(|\mathbf{x}|\right) \right) & \text{if} \quad x_1 > 0, \\ \left(\operatorname{sgn}[\partial_{t^-}\sigma(0)], \ \mathsf{O}\left(|\mathbf{x}|\right) \right) & \text{if} \quad x_1 < 0. \end{cases} \tag{13}$$

The intersection of the hyperplane $x_1 = 0$ and the hyperplane $x_2 = 0$ is an $n-2$ dimensional surface, coordinatized by some $x_3, ..., x_n$, that remain to be chosen. We can choose a basis of these coordinates that is normal to the flow at $\hat{\mathbf{x}} = 0$. Let $y_3, ..., y_n$, be any $n-2$ coordinates orthogonal to x_1, x_2, then let

$$x_i = y_i + \alpha_i(\mathbf{x})\sigma(\mathbf{x}) + \varphi(\mathbf{x})\partial_{t^+}\sigma(\mathbf{x}) \qquad \text{for} \quad i = 3, 4, ... \tag{14}$$

where $\alpha_i = -\left(\partial_{t^-}y_i + \varphi\partial_{t^-}\partial_{t^+}\sigma\right)/\left(\partial_{t^-}\sigma\right)$ and $\varphi = -\left(\partial_{t^+}y_i\right)/\left(\partial^2_{t^+}\sigma\right)$. Applying the derivatives $\partial_{t^\pm}$ gives

$$\frac{d}{dt}x_i = \begin{cases} \boldsymbol{\varepsilon}_i^+\cdot\mathbf{x} & \text{if} \quad x_1 > 0, \\ \boldsymbol{\varepsilon}_i^-\cdot\mathbf{x} & \text{if} \quad x_1 < 0, \end{cases} + \mathsf{O}\left(|\mathbf{x}|^2\right) = \mathsf{O}\left(|\mathbf{x}|\right) \tag{15}$$

where (again omitting the argument $\mathbf{x}$)

$$\boldsymbol{\varepsilon}_i^+ = \left(\partial_{t^+}\alpha_i - (\alpha_i + \partial_{t^+}\varphi)\tfrac{\partial_{t^+}\gamma}{\gamma}, \ \alpha_i + \partial_{t^+}\varphi, \ 0, \ 0, ... \right)/\gamma,$$
$$\boldsymbol{\varepsilon}_i^- = \left(\partial_{t^-}\alpha_i + \tfrac{(\partial_{t^-}\partial_{t^+}\sigma)\partial_{t^-}\varphi}{\partial_{t^-}\sigma}, \ \tfrac{\partial_{t^-}\varphi}{\gamma}, \ 0, \ 0, \ ... \right) ,$$

and since $\frac{d}{dt}x_i = \mathsf{O}\left(|\mathbf{x}|\right)$, this completes the result (8). □

By the implicit function theorem there exists an open set

$$\{(x_1, ..., x_n) : x_1 = x_2 = 0\}$$

of fold points, in a region around $\hat{\mathbf{x}}$ on which $\partial^2_{t^+}\sigma(\mathbf{x})$ and $\partial_{t^-}\sigma(\mathbf{x})$ remain nonzero. Exploring the permutations of the signs of $\partial^2_{t^+}\sigma$ and $\partial_{t^-}\sigma$ in (8) produces the four topologically distinct cases in figure 4. The sign of $\partial^2_{t^+}\sigma$ determines whether the upper flow curves towards or away from the surface at the fold, and the sign of $\partial_{t^-}\sigma$ determines whether the lower flow points towards or away from the surface. The singularity at $x_1 = x_2 = 0$ is not a stationary point of the flow (i.e. $\frac{d}{dt}\mathbf{x} \neq 0$, or more correctly since (2) is set-valued, $0 \notin \frac{d}{dt}\mathbf{x}$).

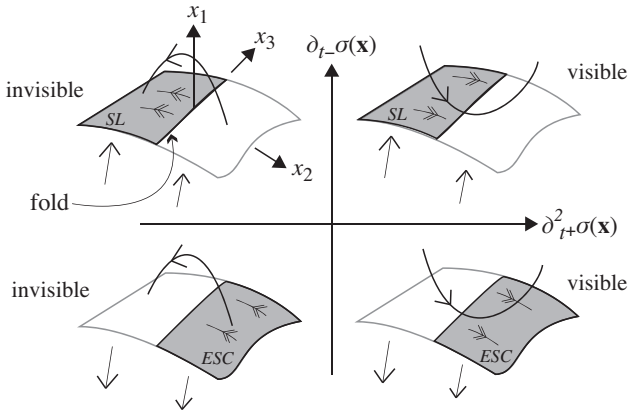

Figure 4: Folds are visible or invisible, and separate regions of sliding (SL, shaded) or escaping (ESC, shaded) from crossing (unshaded). The term *visible* [or *invisible*] identifies a flow curving away from [or towards] the discontinuity surface.

At the fold, the sliding vectors $\partial_{t^s}\mathbf{x}$ found using (5) reduce simply to $\partial_{t^+}\mathbf{x}$, and therefore typically passes through the fold in finite time. The geometry summarized in the expressions above is not only useful for local dynamics, but has been used to study global bifurcations by deriving the so-called *discontinuity mappings* for sliding bifurcations [11], classifying the topologies of sliding bifurcations [4, 16], and computing invariant manifolds at sliding/escaping boundaries [5, 6].

In systems of n dimensions, a pair of $n-2$ dimensional fold sets (one given by each of (6) and (7)) may intersect under generic circumstances. Since each inhabits the $n-1$ dimensional discontinuity surface, such an intersection has dimension $n-3$, and is therefore typical only in $n \geq 3$ dimensions. Such an intersection is known as a two-fold singularity, as explored in the remainder

of this paper. Breaking the inequalities in (6)-(7) permits contact of higher than quadratic order; we do not explore these here, but for two or three dimensional flows see [16, 17, 20].

4 The two-fold

Definition 4. *A two-fold singularity is a set of points* $\hat{\mathbf{x}}$ *where*

$$\sigma(\hat{\mathbf{x}}) = \partial_{t^+}\sigma(\hat{\mathbf{x}}) = \partial_{t^-}\sigma(\hat{\mathbf{x}}) = 0, \tag{16}$$

subject to three non-degeneracy conditions:

$$\partial^2_{t^\pm}\sigma(\hat{\mathbf{x}}) \neq 0 \tag{17}$$

$$\partial_{\mathbf{x}}\sigma(\hat{\mathbf{x}}),\ \partial_{\mathbf{x}}\partial_{t^+}\sigma(\hat{\mathbf{x}}),\ \partial_{\mathbf{x}}\partial_{t^-}\sigma(\hat{\mathbf{x}}) \quad \textit{are linearly independent} \tag{18}$$

$$(\partial_{t^\lambda}\hat{\mathbf{x}}) \cdot (\partial_{\mathbf{x}}\partial_{t^\pm}\sigma(\hat{\mathbf{x}})) \neq 0 \qquad \forall \lambda \in [0,1] \tag{19}$$

where ∂_{t^λ} *is defined in (1).*

Condition (17) says that tangencies between the discontinuity surface and the flow are of quadratic order, while (18) means that the pair of folds (one with respect to each of the upper and lower flows) are transversal. The final condition, (19), means that all values of the linear combination $\partial_{t^\lambda}\mathbf{x}$ have a non-zero component in the plane of $\partial_{t^+}\mathbf{x}$ and $\partial_{t^-}\mathbf{x}$ at $\hat{\mathbf{x}}$. An important consequence of (18)-(19) is that $0 \notin \frac{d}{dt}\mathbf{x}$, so the flow is not stationary at the singularity, yet *how* the flow traverses the singularity turns out to be non-trivial.

The flow curvature with respect to the discontinuity surface is characterized by two functions

$$v^+(\mathbf{x}) := \frac{\partial_{t^+}\partial_{t^-}\sigma(\mathbf{x})}{\sqrt{|\partial^2_{t^+}\sigma(\mathbf{x})\partial^2_{t^-}\sigma(\mathbf{x})|}} \quad \& \quad v^-(\mathbf{x}) := \frac{-\partial_{t^-}\partial_{t^+}\sigma(\mathbf{x})}{\sqrt{|\partial^2_{t^+}\sigma(\mathbf{x})\partial^2_{t^-}\sigma(\mathbf{x})|}}. \tag{20}$$

These are important for classifying all aspects of the local dynamics, and we define their values at the singularity as a pair of constants

$$\nu^+ := v^+(\hat{\mathbf{x}}) \qquad \& \qquad \nu^- := v^-(\hat{\mathbf{x}})\ . \tag{21}$$

We now introduce our main result.

Theorem 2. On the two-fold normal form. *Let the point* $\hat{\mathbf{x}} = 0$ *be a two-fold singularity on a discontinuity surface* $\sigma(\mathbf{x}) = 0$. *Then there exist coordinates* $\mathbf{x} = (x_1, ..., x_n)$ *in which the vector field is given by*

$$\left.\begin{array}{rcl} \frac{d}{dt}(x_1, x_2, x_3) & = & \left\{ \begin{array}{ll} \left(-x_2, -\mathrm{sgn}\left[\partial^2_{t^+}\sigma(0)\right], \nu^+\right) & \text{if} \quad x_1 > 0, \\ \left(\ x_3\ ,\ \nu^-,\ \mathrm{sgn}\left[\partial^2_{t^-}\sigma(0)\right]\ \right) & \text{if} \quad x_1 < 0, \end{array} \right. \\ & & + \quad \left\{ \begin{array}{ll} (0,\ \mathsf{O}(|\mathbf{x}|)\,,\ \mathsf{O}(|\mathbf{x}|)) & \text{if} \quad x_1 > 0, \\ (0,\ \mathsf{O}(|\mathbf{x}|)\,,\ \mathsf{O}(|\mathbf{x}|)) & \text{if} \quad x_1 < 0. \end{array} \right. \\ \frac{d}{dt}x_i & = & \mathsf{O}(|\mathbf{x}|) \qquad \text{for } i = 4, 5, ..., n, \end{array}\right\} \tag{22}$$

Proof of Theorem 2. Define coordinates $\mathbf{x} = (x_1, ..., x_n)$ in which the first three variables are given by

$$x_1 = \alpha\sigma(\mathbf{x}), \quad x_2 = -\beta(\mathbf{x})\partial_{t^+}(\alpha(\mathbf{x})\sigma(\mathbf{x})), \quad x_3 = \frac{\partial_{t^-}(\alpha(\mathbf{x})\sigma(\mathbf{x}))}{\beta(\mathbf{x})}, \tag{23}$$

where

$$\alpha = |\partial^2_{t^+}\sigma\partial^2_{t^-}\sigma|^{-1/2}, \qquad \beta = |\partial^2_{t^-}\sigma/\partial^2_{t^+}\sigma|^{1/4}. \tag{24}$$

The functions α and β are well-defined because the derivatives $\partial^2_{t^\pm}\sigma$ are nonvanishing by (17), and by (18) the variables x_1, x_2, x_3, are linearly independent at the origin, and form a valid coordinate system. The $n-3$ dimensional manifold

$$\{(x_1, ..., x_n) :\ x_1 = x_2 = x_3 = 0\}$$

is a two-fold singularity, and the coordinates $x_4, ..., x_n$ remain to be chosen. Before we define those, simply rearranging (23) gives the dynamics on the first variable,

$$\partial_{t^+}x_1 = -x_2/\beta(\mathbf{x}), \qquad \partial_{t^-}x_1 = x_3\beta(\mathbf{x}). \tag{25}$$

Applying the derivative operators $\partial_{t^\pm}$ from (2) to the next two coordinates, x_2 and x_3, gives (omitting arguments $\mathbf{x}$)

$$\left.\begin{array}{rcl} \dfrac{d}{dt}(x_1, x_2, x_3) & = & \left\{ \begin{array}{ll} \left(-x_2, -\alpha\beta^2\partial^2_{t^+}\sigma\ , \alpha\partial_{t^+}\partial_{t^-}\sigma\right)/\beta & \text{if} \quad x_1 > 0, \\ \left(\ x_3\ , -\alpha\partial_{t^-}\partial_{t^+}\sigma, \alpha\beta^{-2}\partial^2_{t^-}\sigma\right)\beta & \text{if} \quad x_1 < 0, \end{array} \right. \\ & & + \quad \left\{ \begin{array}{ll} \left(0,\ \mathbf{x}\cdot\boldsymbol{\varepsilon}^+_2,\ \mathbf{x}\cdot\boldsymbol{\varepsilon}^+_3\right) & \text{if} \quad x_1 > 0, \\ \left(0,\ \mathbf{x}\cdot\boldsymbol{\varepsilon}^-_2,\ \mathbf{x}\cdot\boldsymbol{\varepsilon}^-_3\right) & \text{if} \quad x_1 < 0, \end{array} \right. \end{array}\right\} \tag{26}$$

where some re-arrangement of derivatives yields

$$\begin{aligned}
\boldsymbol{\varepsilon}_2^+ &= \left(\alpha\beta\partial_{t^+}^2\tfrac{1}{\alpha} \ , \tfrac{1}{\alpha^2\beta}\partial_{t^+}(\alpha^2\beta), \quad 0 \quad , \ 0,0,... \right), \\
\boldsymbol{\varepsilon}_3^+ &= \left(-\tfrac{\alpha}{\beta}\partial_{t^+}\partial_{t^-}\tfrac{1}{\alpha}, \ -\tfrac{1}{\alpha\beta^2}\partial_{t^-}\alpha \ , \ \tfrac{\beta}{\alpha}\partial_{t^+}\tfrac{\alpha}{\beta} \ , \ 0,0,... \right), \\
\boldsymbol{\varepsilon}_2^- &= \left(\alpha\beta\partial_{t^-}\partial_{t^+}\tfrac{1}{\alpha} \ , \ \tfrac{1}{\alpha\beta}\partial_{t^-}(\alpha\beta) \ , -\tfrac{\beta^2}{\alpha}\partial_{t^+}\alpha, \ 0,0,... \right), \\
\boldsymbol{\varepsilon}_3^- &= \left(-\tfrac{\alpha}{\beta}\partial_{t^-}^2\tfrac{1}{\alpha} \ , \quad 0 \quad , \ \tfrac{\beta}{\alpha^2}\partial_{t^-}\tfrac{\alpha^2}{\beta}, \ 0,0,... \right),
\end{aligned}$$

noting that α, β, and $\boldsymbol{\varepsilon}_i^{\pm}$ are all functions of $\mathbf{x}$. As in the proof of Theorem 1, we can apply a time rescaling $t \mapsto t/\mu$ provided that μ is strictly positive. Let $\mu = 1/\beta$ for $x_1 < 0$ and $\mu = \beta$ for $x_1 > 0$, given $\beta > 0$ by (24). Applying $t \mapsto t/\mu$ to (26) we then have

$$\begin{aligned}
\frac{d}{dt}(x_1,x_2,x_3) \ = \ & \begin{cases} \left(-x_2, -\mathrm{sgn}[\partial_{t^+}^2\sigma(\mathbf{x})] \, , v^+(\mathbf{x})\right) & \text{if} \quad x_1 > 0, \\ \left(x_3 \ , \ \ v^-(\mathbf{x}), \ \mathrm{sgn}[\partial_{t^-}^2\sigma(\mathbf{x})] \ \right) & \text{if} \quad x_1 < 0, \end{cases} \\
& + \begin{cases} \left(0, \ \mathbf{x}\cdot\boldsymbol{\varepsilon}_2^+(\mathbf{x}), \ \mathbf{x}\cdot\boldsymbol{\varepsilon}_3^+(\mathbf{x})\right)\beta(\mathbf{x}) & \text{if} \quad x_1 > 0, \\ \left(0, \ \mathbf{x}\cdot\boldsymbol{\varepsilon}_2^-(\mathbf{x}), \ \mathbf{x}\cdot\boldsymbol{\varepsilon}_3^-(\mathbf{x})\right)/\beta(\mathbf{x}) & \text{if} \quad x_1 < 0, \end{cases}
\end{aligned} \tag{27}$$

in terms of the functions $v^{\pm}$ defined in (20), using the fact that $\alpha = 1/|\partial_{t^+}^2\sigma\partial_{t^-}^2\sigma|^{1/2}$, $\alpha\beta^2 = 1/|\partial_{t^+}^2\sigma|$, and $\alpha\beta^{-2} = 1/|\partial_{t^-}^2\sigma|$ by (24). Expanding (27) in powers of $x_1, x_2, ..., x_n$, about the point $\hat{\mathbf{x}} = 0$, the vector field becomes

$$\begin{aligned}
\frac{d}{dt}(x_1,x_2,x_3) \ = \ & \begin{cases} \left(-x_2, -\mathrm{sgn}\left[\partial_{t^+}^2\sigma(0)\right], v^+(0)\right) & \text{if} \quad x_1 > 0, \\ \left(x_3 \ , \ \ v^-(0), \ \ \mathrm{sgn}\left[\partial_{t^-}^2\sigma(0)\right] \right) & \text{if} \quad x_1 < 0, \end{cases} \\
& + \quad \begin{cases} \left(0, \ \mathsf{O}\left(|\mathbf{x}|\right), \ \mathsf{O}\left(|\mathbf{x}|\right)\right) & \text{if} \quad x_1 > 0, \\ \left(0, \ \mathsf{O}\left(|\mathbf{x}|\right), \ \mathsf{O}\left(|\mathbf{x}|\right)\right) & \text{if} \quad x_1 < 0. \end{cases}
\end{aligned} \tag{28}$$

Finally, the components $dx_{j>3}/dt$ are found as follows. At the point $\hat{\mathbf{x}}$ inside the two-fold, the flow switches between two directions, say $\partial_{t^+}\mathbf{x}$ and $\partial_{t^-}\mathbf{x}$ evaluated at $\mathbf{x} = \hat{\mathbf{x}}$, which by (19) are linearly independent; let us call these two vectors $\mathbf{e}_+$ and $\mathbf{e}_-$. Orthogonal to $\mathbf{e}_+$, $\mathbf{e}_-$, and $\partial_{\mathbf{x}}\sigma$, there exist $n-3$ mutually orthogonal unit vectors $\mathbf{e}_i$, $i = 4, ..., n$, which we can take as the bases of coordinates $x_4, ..., x_n$. Then $dx_i/dt = 0$ at $\hat{\mathbf{x}} = 0$, and we have

$$\frac{d}{dt}x_i = \begin{cases} \mathbf{a}_i^+\cdot\mathbf{x} & \text{if} \quad x_1 > 0, \\ \mathbf{a}_i^-\cdot\mathbf{x} & \text{if} \quad x_1 < 0, \end{cases} + \mathsf{O}\left(|\mathbf{x}|^2\right), \tag{29}$$

for $i = 4, 5, ..., n$, where $\mathbf{a}_i^{\pm}$ are vector constants $\mathbf{a}_i^{\pm} = \partial_{\mathbf{x}}\partial_{t^{\pm}}x_i|_{\mathbf{x}=0}$. Since $\frac{d}{dt}x_i = \mathsf{O}\left(|\mathbf{x}|\right)$, this completes (22).

□

By expanding (23) to give $x_2 = -\beta\sigma\partial_{t^+}\alpha - \beta\alpha\partial_{t^+}\sigma$ and $x_3 = \gamma\sigma\partial_{t^-}\alpha + \gamma\alpha\partial_{t^-}\sigma$, we see that the role of x_1, x_2, x_3, is as follows: the $n-1$ dimensional manifold $x_1 = 0$ is the discontinuity surface where $\sigma = 0$, the $n-2$ dimensional manifold $x_1 = x_2 = 0$ is a fold where $\sigma = \partial_{t^+}\sigma = 0$ (see (6)), and the $n-2$ dimensional manifold $x_1 = x_3 = 0$ is a fold where $\sigma = \partial_{t^-}\sigma = 0$ (see (7)).

We can solve the normal form system to give:

Corollary 3. *Trajectories of (22) are arc segments of the form*

$$\left.\begin{array}{l} x_1(t) = x_1(0) - tx_2(0) + \frac{1}{2}\mathrm{sgn}[\partial^2_{t^+}\sigma(0)]t^2 + \mathsf{O}\left(t^3\right) \\ x_2(t) = x_2(0) - \mathrm{sgn}[\partial^2_{t^+}\sigma(0)]t + \mathsf{O}\left(t^2\right) \\ x_3(t) = x_3(0) + \nu^+ t + \mathsf{O}\left(t^2\right) \end{array}\right\} \tag{30}$$

for $x_1(0) \geq 0$ provided $x_1(t) \geq 0$, and

$$\left.\begin{array}{l} x_1(t) = x_1(0) + tx_3(0) + \frac{1}{2}\mathrm{sgn}[\partial^2_{t^-}\sigma(0)]t^2 + \mathsf{O}\left(t^3\right) \\ x_2(t) = x_2(0) + \nu^- t + \mathsf{O}\left(t^2\right) \\ x_3(t) = x_3(0) + \mathrm{sgn}[\partial^2_{t^-}\sigma(0)]t + \mathsf{O}\left(t^2\right) \end{array}\right\} \tag{31}$$

for $x_1(0) \leq 0$ provided $x_1(t) \leq 0$. In both cases we have $x_i(t) = x_i(0) + \mathsf{O}\left(t^2\right)$ for $i = 4, 5, ..., n$.

Proof. Expand the trajectories $(x_1(t), x_2(t), ...)$ of (22) as a power series in t, namely $x_i(t) = x_i(0) + t\frac{dx_i(0)}{dt} + \frac{1}{2}t^2\frac{d^2x_i(0)}{dt^2} + ...$, substituting in $d^r x_i/dt^r$, found from (11), to obtain separate expansions in $x_1 > 0$ and $x_1 < 0$. These expansions yield (30) and (31) respectively, along with $x_i(t) = x_i(0) + \mathsf{O}\left(t^2\right)$ for $i = 4, 5, ..., n$. □

In (30)-(31) we express $x_1(t)$ to $\mathsf{O}\left(t^2\right)$, but only express $x_2(t)$ and $x_3(t)$ to $\mathsf{O}\left(t\right)$, for later use: these will be sufficient to obtain the correct dependence on terms quadratic in x_2 and x_3 when both t and $\mathbf{x}$ are considered to be small.

In the following sections we explore the classes of behaviour generated by the normal form (22). The key point to note from Corollary 3 is that the leading order dynamics of $x_1(t), x_2(t), x_3(t)$, is independent of the variables $x_4, x_5, \ldots, x_n$, which allows us to form a classification based purely upon the dynamics of x_1, x_2, x_3.

The variables $x_4, x_5, ..., x_n$, do have a role to play, of course, because they enter into the values of the parameters $\nu^\pm$ and $\partial^2_{t^\pm}\sigma(0)$, which depend on the point $\hat{\mathbf{x}} = (\hat{x}_1, \hat{x}_2, ..., \hat{x}_n)$ at which the expression (22) is derived. At any given point, the possible signs of the derivatives $\partial^2_{t^\pm}\sigma(0)$ give one of three

topological flavours of two-fold (figure 5), and the values of the parameters $\nu^{\pm}$ divide these further into dynamical subclasses. Different values thus determine neighbourhoods of different points $\mathbf{x} \in \mathbb{R}^n$ with different dynamics, which we describe in sections 5.1-5.3. The transition between such regions occurs where the non-degeneracy conditions (17)-(19) break down at critical values of $\partial^2_{t^{\pm}}\sigma$ and $\nu^{\pm}$, and this requires study of the higher order terms labelled $\mathsf{O}(|\mathbf{x}|)$ in (22). We leave the rich problem of the dynamics arising from these transitions to further work.

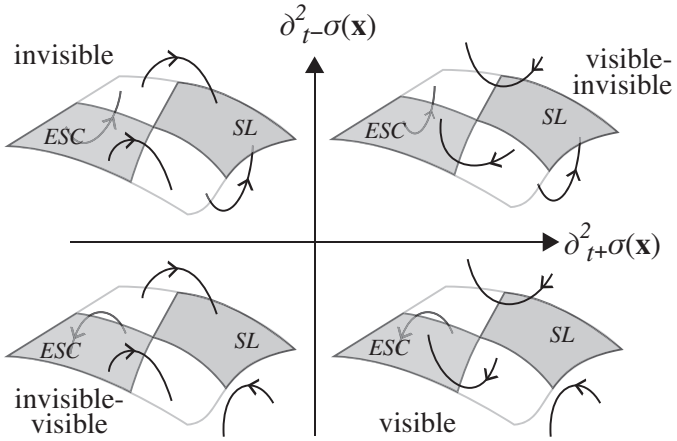

Figure 5: Two-folds come in three flavours depending on whether the folds that comprise them are visible or invisible (the top-right and bottom-left cases are topologically equivalent), as determined by the signs of $\partial^2_{t^{\pm}}\sigma$. Regions of sliding ($SL$, shaded), escaping ($ESC$, shaded), and crossing (unshaded) all meet at the singularity.

In three dimensions, (22) is equivalent to normal forms for the two-fold that have appeared previously in [13, 19, 20] and more recently in [7, 15], up to a variety of sign conventions, for which the result (22) above has the benefit of having a single unified form. The remainder of this section sets out the principles of sliding and crossing in the local expression (22).

4.1 Sliding near a two-fold

The time derivative along the sliding flow on $x_1 = 0$ is obtained by substituting (22) into (2), giving

$$\left.\begin{aligned} \partial_{t^s} x_1 &= 0, \\ \partial_{t^s} x_2 &= \left(\nu^- x_2 - \operatorname{sgn}\left[\partial^2_{t^+}\sigma(0)\right] x_3\right) / (x_2 + x_3) + \mathsf{O}(|\mathbf{x}|), \\ \partial_{t^s} x_3 &= \left(\operatorname{sgn}\left[\partial^2_{t^-}\sigma(0)\right] x_2 + \nu^+ x_3\right) / (x_2 + x_3) + \mathsf{O}(|\mathbf{x}|), \\ \partial_{t^s} x_i &= \mathsf{O}(|\mathbf{x}|), \qquad i = 4, 5, \ldots, n. \end{aligned}\right\} \tag{32}$$

The righthand side of (32) is independent of the coordinates $x_4, x_5, \ldots$. The dynamics in the x_2 and x_3 directions is thus given, to leading order, by the two-dimensional system

$$\partial_{t^s}(x_2, x_3) = \frac{(x_2, x_3)}{x_2 + x_3} \cdot \begin{pmatrix} \nu^- & \operatorname{sgn}\left[\partial^2_{t^-}\sigma(0)\right] \\ -\operatorname{sgn}\left[\partial^2_{t^+}\sigma(0)\right] & \nu^+ \end{pmatrix}. \tag{33}$$

The 2×2 matrix in (33) has determinant

$$D = \operatorname{sgn}\left[\partial^2_{t^+}\sigma(0)\partial^2_{t^-}\sigma(0)\right] + \nu^+\nu^- \tag{34}$$

and trace

$$T = \nu^+ + \nu^- \,. \tag{35}$$

These, and the eigenvectors of the 2×2 matrix, are sufficient to determine the phase portrait of the sliding flow (see for example [13, 15]). Essentially, the factor $\frac{1}{x_2+x_3}$ amounts to a time-scaling, albeit one that is singular at the two-fold. Neglecting this factor, the phase portrait of (33) resembles a simple equilibrium at $(x_2, x_3) = 0$, and will have degeneracies where the determinant (34) and trace (35) vanish. Although the full vector field does not have an equilibrium at $(x_2, x_3) = 0$ (recall from the paragraph following (19) that $\frac{d}{dt}\mathbf{x} = 0$ is not a permitted vector there), these still constitute degeneracies of the piecewise-smooth flow. The complete family of distinct phase portraits are explored in section 5. One particular result will appear repeatedly in sections 5.1-5.3, given by the following corollary to Theorem 2.

Corollary 4. *The determinant (34) is non-zero by condition (19). Therefore $D = 0$ constitutes a degeneracy of the two-fold, and corresponds to a parameter curve where*

$$D = \operatorname{sgn}[\partial^2_{t^+}\sigma(0)]\operatorname{sgn}[\partial^2_{t^-}\sigma(0)] + \nu^+\nu^- = 0 \tag{36}$$

subject to

$$\frac{\nu^-}{\operatorname{sgn}[\partial^2_{t^+}\sigma(0)]+\nu^-} \in [0,1] \qquad \text{and} \qquad \frac{\operatorname{sgn}(\partial^2_{t^-}\sigma)}{\operatorname{sgn}[\partial^2_{t^-}\sigma(0)]-\nu^+} \in [0,1] \,. \tag{37}$$

Proof. To show this we prove that (19) reduces to $D \neq 0$ in the normal form. Condition (19) means that $\partial_{t^\lambda}\mathbf{x}$ has a non-zero component in the plane of $\partial_{\mathbf{x}}\partial_{t^+}\sigma$ and $\partial_{\mathbf{x}}\partial_{t^-}\sigma$, at $\hat{\mathbf{x}}$, for all $\lambda \in [0,1]$. In the normal form (22) the gradient vectors $\partial_{\mathbf{x}}\partial_{t^+}\sigma$ and $\partial_{\mathbf{x}}\partial_{t^-}\sigma$ correspond to the x_2 and x_3 directions, so (19) states that the second and third components of $\partial_{t^\lambda}\mathbf{x} =$

$\lambda\partial_{t^+}\mathbf{x} + (1-\lambda)\partial_{t^-}\mathbf{x}$ are nonzero. Evaluating these, and eliminating λ, gives $\mathrm{sgn}[\partial^2_{t^+}\sigma(0)]\mathrm{sgn}[\partial^2_{t^-}\sigma(0)] + \nu^+\nu^- \neq 0$, which is $D \neq 0$ by (34). Solving for λ and substituting into the requirement $\lambda \in [0,1]$ gives (37). Thus $D \neq 0$ is violated on a parameter curve $\nu^+\nu^- = \pm 1$ from (36), with restrictions on the signs of $\nu^\pm$ as implied in (37).

□

The sliding and escaping regions (given by (4)) in the normal form occupy $x_2x_3 > 0$ on $x_1 = 0$, implying $x_2+x_3 > 0$ in the sliding region and $x_2+x_3 < 0$ in the escaping region, in both of which the system (32) is well-defined. The sliding vector field is not well-defined at the two-fold singularity itself (nor on the line $x_2+x_3 = 0$, but this passes through the crossing regions), where both the numerator and denominator of (32) vanish. So (32) specifies the sliding flow in the neighbourhood of the singularity, excepting the singularity itself. What happens when the sliding flow intersects the singularity is discussed in section 4.2 below.

4.2 Sliding through a two-fold: canards

What happens if a trajectory satisfying (33) arrives at the singularity, where (33) is undefined?

The failure of (33) occurs because every vector $\partial_{t^\lambda}\mathbf{x} \in \frac{d}{dt}\mathbf{x}$ lies tangent to the discontinuity surface at the singularity, so none can be distinguished uniquely as the vector $\partial_{t^s}\mathbf{x}$ defining a sliding flow. However, when the genericity conditions (17)-(19) are satisfied at the singularity, all vectors in the set $\frac{d}{dt}\mathbf{x}$ are non-zero. This means that a trajectory that intersects the singularity must pass through it in finite time. In doing so the flow passes from the sliding region to the escaping region, or vice versa. Trajectories consistent with definition 2 are formed by concatenating the two flows (similar to concatenating the upper and lower flows at a crossing region), with their tangent vectors switching between different values of ∂_{t^s} given by (5).

One possibility is then that the flow is conveyed *from* sliding *to* escaping, via the singularity. Such trajectories have been termed *canards* [8], borrowing a term from slow-fast systems [2] and inspired by the French term 'canard', alluding to the counterintuitive nature of such dynamics. *Faux canards* are similar but travel in the opposite, prointuitive, direction, from escaping to sliding regions.

One must then recall that a point in the sliding region can be reached from many points in the piecewise-smooth flow, including a unique sliding trajectory $\mathbf{x}_s(t)$ with tangent vector (33), and a continuum of trajectories

that impact the discontinuity surface along $\mathbf{x}_s(t)$ (figure 6, left). We say that such a point has many possible histories in the flow. Similarly, a point in the escaping region has many possible futures, consisting of a unique sliding trajectory $\mathbf{x}_s(t)$ with tangent vector (33), and a continuum of trajectories that depart the discontinuity surface from points along $\mathbf{x}_s(t)$. The two-fold singularity compounds this multi-valuedness because it lies on the boundary of both sliding and escaping regions (figure 7).

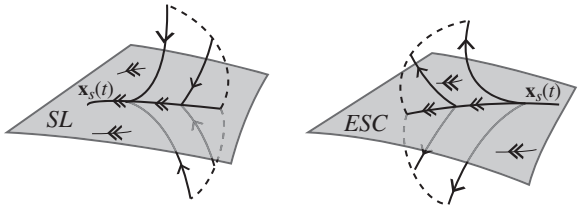

Figure 6: Non-unique histories or futures: a point in the sliding region (SL) can be reached by many trajectories, while a point in the escaping region (ESC) evolves into many trajectories.

In section 5 (figures 8, 9, 10), two-folds are shown to exhibit different canard topologies: there may be no canards (the flow avoids the singularity), or the family of canards may form either an $n-1$ dimensional set (figure 7(i)), or an n dimensional set (figure 7(ii)). The latter are robust in the sense that there exist open sets of initial conditions in $\mathbb{R}^n$ whose trajectory intersects the two-fold.

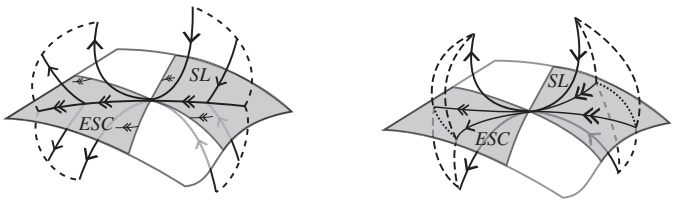

Figure 7: Simple canards and robust canards from sliding (SL) to escaping (ESC). Simple canards (left) form an $n-1$ dimensional set, and robust canards (right) form an n dimensional set. In any number of dimensions $n \geq 3$, the normal form variables x_1, x_2, x_3, follow the phase portraits shown. Examples of the simple canards are found in figure 8(i) and figures 9(v-vii), examples of the robust canards are found in figures 9(iii-iv) and figure 10(iii).

4.3 The crossing map around an invisible fold

If $\partial^2_{t^+}\sigma(0) < 0$ then the fold set $\sigma = \partial_{t^+}\sigma = 0$ is invisible, so the upper flow (30) forms arcs curved towards the discontinuity surface. Similarly if $\partial^2_{t^-}\sigma(0) < 0$ then the fold set $\sigma = \partial_{t^-}\sigma = 0$ is invisible, and the lower flow (31) forms arcs curving towards the surface.

Each of these induces a return map on the discontinuity surface, found by eliminating t in each system (30) or (31), and seeking the terminal points of trajectories on $x_1 = 0$. Thus near an invisible fold, a point

$$(x_1(0), x_2(0), x_3(0), ...) = (0, \xi_2, \xi_3, ...)$$

with $\xi_2 < 0$ will map via the $x_1 > 0$ flow (30) according to

$$\begin{pmatrix} \xi_2 \\ \xi_3 \end{pmatrix} \mapsto B^+ \begin{pmatrix} \xi_2 \\ \xi_3 \end{pmatrix} + \mathsf{O}\left(|\boldsymbol{\xi}|^2\right), \quad B^+ = \begin{pmatrix} -1 & 0 \\ -2\nu^+ & 1 \end{pmatrix}, \tag{38}$$

while a point with $\xi_3 < 0$ will map via the $x_1 < 0$ flow (31) according to

$$\begin{pmatrix} \xi_2 \\ \xi_3 \end{pmatrix} \mapsto B^- \begin{pmatrix} \xi_2 \\ \xi_3 \end{pmatrix} + \mathsf{O}\left(|\boldsymbol{\xi}|^2\right), \quad B^- = \begin{pmatrix} 1 & -2\nu^- \\ 0 & -1 \end{pmatrix}. \tag{39}$$

The maps (38) and (39) form the basis of all studies of crossing dynamics local to a two-fold with invisible tangencies. Their local independence of the coordinates $\xi_4, \xi_5, ...$, is key, permitting a classification to be formed in terms of dynamics in the (ξ_2, ξ_3) plane only.

The domains of the two maps, respectively $\xi_2 < 0$ and $\xi_3 < 0$, overlap in the escaping region $\xi_2, \xi_3 < 0$. Also their ranges, respectively $\xi_2 > 0$ and $\xi_3 > 0$, overlap in the sliding region $\xi_2, \xi_3 > 0$. Trajectories switch from one map to the other in the crossing regions $\xi_2\xi_3 < 0$: points in $\xi_2 < 0 < \xi_3$ lie in the range of (39) and the domain of (38), while points in $\xi_3 < 0 < \xi_2$ lie in the range of (38) and the domain of (39). The folds lie on $\xi_2 = 0$ or $\xi_3 = 0$, and are fixed points of the maps (38) and (38) respectively.

If both folds are invisible, then there exist trajectories of (22) that wind around the two-fold many times, by switching between the upper and lower flows, crossing the discontinuity surface at a sequence of points given by repeatedly applying the maps (38) and (39) in turn. To study a sequence of such crossings, one has a useful expression for the $2m^{th}$ return maps,

$$\begin{aligned} (B^-B^+)^m &= \tfrac{\sin(2mg)}{\sin(2g)} B^-B^+ - \tfrac{\sin(2(m-1)g)}{\sin(2g)} \mathcal{I}, \\ (B^+B^-)^m &= \tfrac{\sin(2mg)}{\sin(2g)} B^+B^- - \tfrac{\sin(2(m-1)g)}{\sin(2g)} \mathcal{I}, \end{aligned}$$

where

$$\nu^+\nu^- = \cos^2 g \tag{40}$$

and $\mathcal{I}$ is the 2×2 identity matrix [12]. The value $\nu^+\nu^- = 1$ constitutes a degeneracy where the maps B^+B^- and B^-B^+ have only one eigenvalue, equal to unity, and by Corollary 4 this corresponds to violation of (19) (since if both folds are invisible then $\text{sgn}[\partial^2_{t^\pm}\sigma(0)]\text{sgn}[\partial^2_{t^\pm}\sigma(0)] = -1$ in (36)).

5 Classification of two-folds

In this section we explore the different classes of two-fold arising from (22), found by the analysis outlined throughout section 4. We summarize key results known for systems of three dimensions [12, 15], showing which aspects of that dynamics are observed in higher dimensions due to the expressions (33)-(39). We will use the terminology from section 4.2, that canards are sliding trajectories that traverse the singularity from sliding to escaping regions, and faux canards are similar but in the reverse direction.

A vital parameter for determining the behaviour at a two-fold singularity is the product of the parameters ν^+ and ν^- defined in (20). The product $\nu^+\nu^-$ appears both in the expressions for sliding dynamics in (34), and for crossing dynamics in (40). It has a simple geometrical interpretation: it quantifies the jump in the vector field at the singularity. It is related to the angle between $\partial_{t^+}\hat{\mathbf{x}}$ and $\partial_{t^-}\hat{\mathbf{x}}$, by the equation

$$\nu^+\nu^- = \alpha\frac{\cot\phi - \cot\theta^+}{\cot\phi - \cot\theta^-}, \qquad |\alpha| = 1, \tag{41}$$

where ϕ measures the angle between the folds, and $\theta^\pm$ measures the angles between the vectors $\partial_{t^\pm}\mathbf{x}$ and the fold sets $\{\mathbf{x} : \partial_{t^\pm}\sigma(\mathbf{x}) = \sigma(\mathbf{x}) = 0\}$. These angles are defined in the plane spanned by $\partial_{t^+}\mathbf{x}$ and $\partial_{t^-}\mathbf{x}$ at the singularity. The term α is $+1$ if both folds are visible or both are invisible, and is -1 if they are mixed. Formulae in terms of flow derivatives are given in Appendix A. In the normal form (22) the pair of folds are orthogonal, so $\phi = \pi/2$ and the angular jump simplifies to

$$\nu^+\nu^- = \alpha\,\tan\theta^-/\tan\theta^+. \tag{42}$$

This reduced formula appeared in [7, 15]. The topologies of so-called visible or invisible two-folds (with $\alpha = +1$) depend on this parameter alone. We will show that only the mixed case, the visible-invisible two-fold (with $\alpha = -1$), demands inspection of ν^+ and ν^- individually.

5.1 The visible two-fold

If $\partial_{t^+}\sigma(0) > 0 > \partial_{t^-}\sigma(0)$ then the two-fold is the intersection of a pair of visible folds. In coordinates $\mathbf{x} = (x_1, x_2, ...)$, to leading order (22) becomes

$$\frac{d}{dt}\mathbf{x} = \begin{cases} (-x_2,\ -1,\ \nu^+,\ 0\ ,\ 0\ , ...) & \text{if} \quad x_1 > 0, \\ (\ x_3\ ,\ \nu^-,\ -1\ ,\ 0\ ,\ 0\ , ...) & \text{if} \quad x_1 < 0, \end{cases} \tag{43}$$

which induces a sliding flow on $\{\mathbf{x} \in \mathbb{R}^n : \; x_1 = 0, \; x_2 x_3 > 0\}$ with vector field (32), which to leading order becomes

$$\partial_{t^s}\mathbf{x} = \left(0, \; \nu^- x_2 - x_3, \; \nu^+ x_3 - x_2, \; 0 \; , \; 0 \; , ...\right) / (x_2 + x_3). \tag{44}$$

The visible two-fold is the simplest to understand, because the intersection between the flow and singularity is rather trivial. The flow curves away from the discontinuity, as seen in the left of figure 8, so that locally trajectories will visit the discontinuity surface at most once. The sliding and escaping regions contain either canards or robust faux canards, as shown in the right of figure 8. This is found by straightforward analysis of the sliding vector field $\partial_{t^s}\mathbf{x}$ above, see [7, 13] for details of the phase portrait in the (x_2, x_3) plane. The delimiting case is $\nu^+\nu^- = 1$ for $\nu^+, \nu^- > 0$ (from Corollary 4).

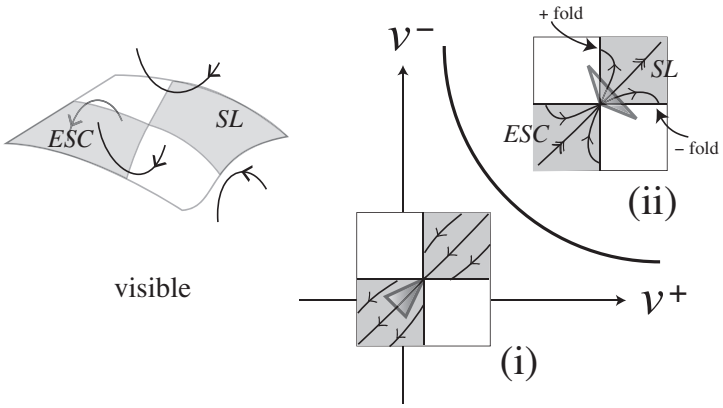

Figure 8: The visible two-fold. Left: the discontinuity manifold is partitioned into sliding (SL) and escaping (ESC) regions (shaded), and crossing regions (unshaded), bounded by visible folds. Right: the $\nu^\pm$ parameter space, showing the transition curve $\nu^+\nu^- = 1$, $\nu^\pm > 0$, and inset: phase portraits of the sliding flow, with different cases: (i) simple canards if $\nu^+\nu^- < 1$ and/or $\nu^+ < 0$ and/or $\nu^- < 0$; (ii) robust faux canards if $\nu^\pm > 0$ and $\nu^+\nu^- > 1$. The set-valued velocity vector is illustrated by a shaded triangle at the singularity.

5.2 The visible-invisible two-fold

If $\partial_{t^\pm}\sigma(0) > 0$ then the two-fold is the intersection of a visible and an invisible fold. In coordinates $\mathbf{x} = (x_1, x_2, ...)$, to leading order (22) becomes

$$\frac{d}{dt}\mathbf{x} = \begin{cases} (-x_2, -1, \; \nu^+, \; 0 \; , \; 0 \; , ...) & \text{if} \quad x_1 > 0, \\ (\; x_3 \; , \nu^-, \; 1 \; , \; 0 \; , \; 0 \; , ...) & \text{if} \quad x_1 < 0. \end{cases} \tag{45}$$

This induces a sliding flow on $\{\mathbf{x} \in \mathbb{R}^n :\ x_1 = 0,\ x_2 x_3 > 0\}$ with vector field (32) which to leading order becomes

$$\partial_{t^s}\mathbf{x} = \left(0,\ \nu^- x_2 - x_3,\ x_2 + \nu^+ x_3,\ 0\ ,\ 0\ , ...\right)/(x_2 + x_3). \tag{46}$$

The sliding and escaping regions can contain canards and faux canards, robust or not, as delimited by the transition curves in figure 9. An explicit

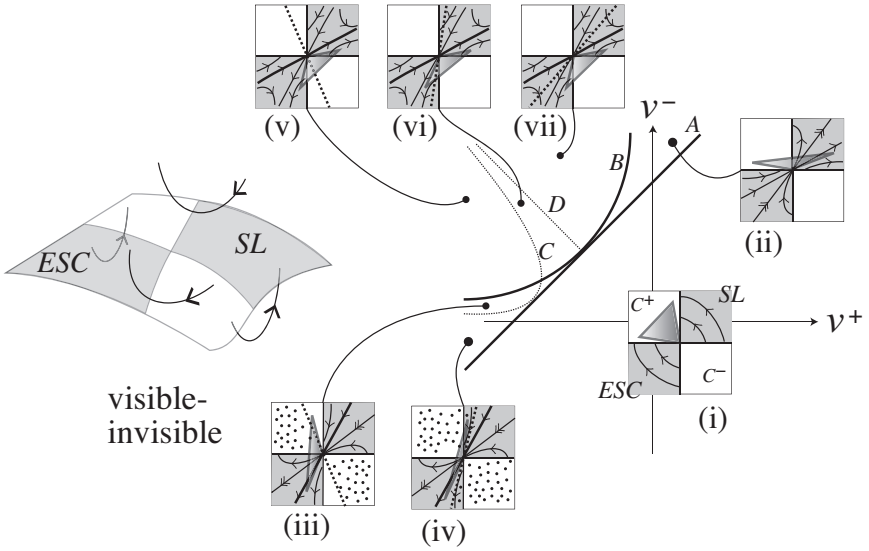

Figure 9: The visible-invisible two-fold. Left: the sliding (SL) and escaping (ESC) regions (shaded), and crossing regions (unshaded), are bounded by one visible and one invisible fold. Right: $\nu^{\pm}$ space showing (inset) phase portraits of the sliding flow, with different cases: (i) no canards; (ii) robust faux canards; (iii-iv) robust canards whose set-valued flow passes through only part (iii) or all (iv) of the crossing regions (dotted); (v-vii) coexisting simple canards and faux canards. The set-valued flow of the faux canard passes through: the crossing regions in (v), the visible fold in (vi), and neither in (vii). Transitions between topologies occur along the line $\nu^+ - \nu^- = -2$, and in $\nu^+ - \nu^- < -2$ along the curves $\nu^+\nu^- = -1$, $2\nu^-(\nu^+ + \nu^-) = -1$, and $\nu^+ = -\nu^-$.

derivation of these curves is a straightforward but lengthy exercise; details are described briefly in [13], and the main features of the sliding vector field are derived in [7]. We outline the key points here. Different types of canards can be present in the sliding and escaping regions, and the type changes along parameter curves $\{\nu^+\nu^- = -1,\ \nu^+ < 0 < \nu^-\}$ and $\{\nu^+ - \nu^- = -2\}$, which correspond to degeneracies associated with the Jacobian of the numerator of the (x_2, x_3) part of (46),

$$J = \begin{pmatrix} \nu^- & -1 \\ 1 & \nu^+ \end{pmatrix},$$

(this is just the 2×2 matrix in (33) with determinant (34) and trace (35), in the case of a visible-invisible two-fold). The curve $\nu^+\nu^- = -1$ is where the determinant of J vanishes (where (19) is violated by Corollary 4). The line $\nu^+ - \nu^- = -2$ is where J has two identical eigenvalues $1+\nu^+$. Two further transition curves in the parameter regime $\nu^+ - \nu^- < -2$ delimit cases where the flow through the faux canards passes either through the crossing regions, the visible fold, or neither: on the curve $2\nu^-(\nu^+ + \nu^-) = -1$ the lower flow (using the map (39)) maps the eigenvector of J associated with the greatest eigenvalue onto the visible fold; on the curve $\nu^+ + \nu^- = 0$ the lower flow (again using (39)) maps the eigenvectors of J onto eachother.

5.3 The Teixeira singularity

If $\partial_{t^-}\sigma(0) > 0 > \partial_{t^+}\sigma(0)$ then the two-fold is the intersection of a pair of invisible folds, also known as the *Teixeira singularity*. In coordinates $\mathbf{x} = (x_1, x_2, ...)$, to leading order (22) becomes

$$\frac{d}{dt}\mathbf{x} = \begin{cases} (-x_2,\ 1,\ \nu^+,\ 0\ ,\ 0\ , ...) & \text{if} \quad x_1 > 0, \\ (\ x_3\ , \nu^-,\ 1\ \ ,\ 0\ ,\ 0\ , ...) & \text{if} \quad x_1 < 0, \end{cases} \tag{47}$$

and the sliding flow on $\{\mathbf{x}\in\mathbb{R}^n :\ x_1 = 0,\ x_2x_3 > 0\}$ has vector field (32) which to leading order becomes

$$\partial_{t^s}\mathbf{x} = \left(0,\ \nu^- x_2 + x_3, x_2 + \nu^+ x_3,\ 0,\ 0, ...\right)/(x_2 + x_3). \tag{48}$$

The invisible two-fold leads to particularly interesting local dynamics, because the flow can return to the discontinuity many times (by repeatedly applying the maps (38)-(39)). Recall from section 2 that the discontinuity surface divides into crossing regions given by (3), sliding regions where $\partial_{t^+}\sigma < 0 < \partial_{t^-}\sigma$ and escaping regions where $\partial_{t^-}\sigma < 0 < \partial_{t^+}\sigma$.

In [15] it was shown that, in 3-dimensional systems, (47) belongs to one of three dynamical classes:

(i) if $\nu^+ > 0$ or $\nu^- > 0$, there exists a simple faux canard, and between ejection from the escaping region to impact on the sliding region the flow crosses the discontinuity surface at most once from $\sigma < 0$ to $\sigma > 0$ if $\nu^+ > 0$, and at most once from $\sigma > 0$ to $\sigma < 0$ if $\nu^- > 0$;

(ii) if $\nu^\pm < 0 < 1 - \nu^+\nu^-$, there exists a simple faux canard, and between ejection from the escaping region to impact on the sliding region the flow crosses the discontinuity surface at least once;

(iii) if $\nu^{\pm} < 0 < \nu^{+}\nu^{-} - 1$, the entire sliding flow consists of robust canards, and the crossing flow traverses the discontinuity repeatedly as it tends asymptotically towards and away from a pair of invariant manifolds (one attracting, one repelling) extending from the singularity.

In [12], case (ii) was supplemented with the result that, if $\nu^{+}\nu^{-} = \cos^2 \frac{\pi}{k+1}$ where $k \geq 2$ is an integer, then the flow crosses the discontinuity exactly k times between ejection from the escaping region to impact on the sliding region. Moreover, if $\nu^{\pm} < 0$ and $\nu^{+}\nu^{-} = \cos^2 \frac{\pi}{r+1}$ but $r > 1$ is not an integer, then between ejection from the escaping region to impact on the sliding region, different parts of the flow cross the discontinuity either k or $k+1$ times, where k and $k+1$ are the integers either side of r. As $k \to \infty$, the transition curves $\nu^{+}\nu^{-} = \cos^2 \frac{\pi}{k+1}$ accumulate onto the particular curve $\nu^{+}\nu^{-} = 1$. On this curve the non-degeneracy condition (19) is violated (as in Corollary 4), therefore the leading order expression (47) is no longer valid.

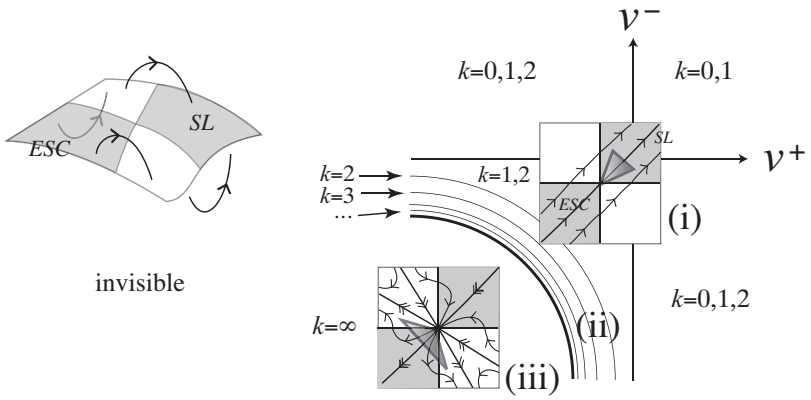

Figure 10: The invisible two-fold. Left: the sliding (SL) and escaping (ESC) regions (shaded), and crossing regions (unshaded), are bounded by invisible folds. Right: the $\nu^{\pm}$ space showing (inset) phase portraits of the sliding flow and the crossing map, with different cases: (i)-(ii) faux canards and crossing numbers k if $\nu^{+}\nu^{-} < 1$ or if ν^{+} or ν^{-} is positive; (iii) robust canards and infinite crossing numbers if $\nu^{\pm} < 0 < \nu^{+}\nu^{-} - 1$.

Originally derived for systems of three dimensions, statements (i)-(iii) hold generally in higher dimensions because they depend solely on the leading order part (47) of the full system (22), which depends only on the (x_1, x_2, x_3) components near the two-fold. That is, (i)-(iii) apply on a neighbourhood where the conditions (16)-(19) are satisfied.

A trajectory may of course evolve in such a way that the higher order terms $\mathsf{O}(|\mathbf{x}|)$ in (22) become significant. It was shown in [7], for example,

that in case (iii), the effect of higher order terms in the vector field is to cause the invariant manifolds (straight lines through the singularity in figure 10, inset (iii)) to curve such they intersect the sliding regions; this effect is significant only near a bifurcation that occurs at $\nu^+\nu^- = 1$, and beyond the scope of the present paper, but worth a brief remark as follows below.

Dynamics at the critical value $\nu^+\nu^- = 1$ has only been studied in detail in three dimensions [7], where a bifurcation of the local flow occurs. By studying the effect of higher order terms as $\nu^+\nu^-$ passes through unity, a stationary point of the sliding flow was shown to pass through the two-fold, accompanied by the appearance of a limit cycle, leading under certain conditions to a non-deterministic kind of chaos. The transition takes the form of the nonsmooth diabolo bifurcation [15, 7], so-called due to the annihilation of an invariant surface resembling a double-cone. The extension of these particular features to higher dimensions is not known.

6 Concluding remarks

Locally the two-fold singularity comes in three flavours, depending on the sign of curvature (the *visibility*) of the flow on either side of the singularity. Each flavour has a number of structurally stable subclasses, which are now understood in considerable detail. A local expansion provides the dynamics in any class as a flow passes close to a two-fold. By virtue of the local analysis presented here, the two-fold's effect on the flow takes place intrinsically in three dimensions, with higher dimensions merely decorating the central structure, and weaving together the different dynamical substructures the flow can exhibit.

This is just the first step in understanding the dynamics of the two-fold. In higher dimensions the two-fold singularity is a set of points, in which different subsets may exhibit different classes of the behaviours shown here. Transitions of the flow between these classes are expected to result in further novel dynamics, and are left to future study.

The interplay of crossing and sliding dynamics can lead to some misunderstanding over the two-fold's attractive/repulsive properties. In short, a two-fold singularity is not generally an invariant set, nor does it contain any stationary points, but forms a bridge between sliding and escaping. This can create a multi-valued flow, because points in the sliding region have many possible histories, while points in the escaping region have many possible futures. Despite this uncertainty, the flow evolves within a well-determined set, defined by the sliding flow and any canards it may contain, concatenated

with the flow outside the discontinuity surface.

Highly degenerate forms of the two-folds occur in systems with symmetries. Like the two-fold, these have a long history in nonsmooth systems [1, 18], and remain a subject of current interest, particularly in electronic control. Typically, in $n > 3$ dimensions or when parameters are varied, one can expect the degeneracy conditions (17)-(19) to be violated at certain points, curves, surfaces, etc., depending on the value of n. For example, an equilibrium may pass through a two-fold [7, 20], a pair of two-folds may collide to form a fold-cusp [20], two-folds may occur at the intersection of multiple discontinuity surfaces, and so on, and of such scenarios, particularly in higher dimensions, little is known.

There has been no study here of global bifurcations. For a flow that arrives at a two-fold singularity, the kind of local approach taken here allows global bifurcations to be characterised in terms of their local interaction with the discontinuity, see for example [16]. These form the elements for ongoing study of how specific global features interact with discontinuities, and a starting point of the hunt for two-folds in physical systems [3, 10, 14].

Acknowledgements. MRJ's research is supported by EPSRC Grant Ref: EP/J001317/1.

A The angular jump parameter v^+v^-

From the definition of $v^\pm$ in (20), we have (omitting arguments $\mathbf{x}$)

$$v^+v^- = -\frac{(\partial_{t^+}\partial_{t^-}\sigma)(\partial_{t^-}\partial_{t^+}\sigma)}{|\partial^2_{t^+}\sigma\partial^2_{t^-}\sigma|} \ .$$

Let $f^\pm = \partial_{t^\pm}\mathbf{x}$, then from the standard definition of Lie derivatives we can substitute $\partial_{t^\pm} = \partial_{t^\pm}\mathbf{x}\cdot\partial_{\mathbf{x}} = f^\pm\cdot\partial_{\mathbf{x}}$, and write

$$\begin{aligned} v^+v^- &= -\frac{(f^+\cdot\partial_{\mathbf{x}}\partial_{t^-}\sigma)(f^-\cdot\partial_{\mathbf{x}}\partial_{t^+}\sigma)}{|(f^+\cdot\partial_{\mathbf{x}}\partial_{t^+}\sigma)(f^-\cdot\partial_{\mathbf{x}}\partial_{t^-}\sigma)|} \\ &= -Q^+_-Q^-_+/|Q^+_+Q^-_-| \end{aligned} \tag{49}$$

where $Q^i_j = f^i\cdot(\partial_{\mathbf{x}}\partial_{t^j}\sigma)$, with i and j denoting the labels $+$ or $-$.

We will express this in terms of angles between the vectors $f^\pm$ and the folds, measured at the singularity. In $\mathbb{R}^n$, we can specify these angles uniquely (up to factors of 2π) if we measure them in the plane spanned by f^+ and f^-. This plane typically intersects the folds, allowing us to measure

angles *from* the folds *to* the vectors $f^{\pm}$. We identify the angle of rotation from f^- to f^+ as positive and measure all angles in this direction. Let us then define

$$\varepsilon_j = Q_j^- f^+ - Q_j^+ f^-, \tag{50}$$

so that the vector ε_j lies in the plane spanned by f^+ and f^-, and also lies in the fold set $\partial_{\mathbf{x}}\partial_{tj}\sigma = 0$ since a short calculation shows $\varepsilon_j \cdot \partial_{\mathbf{x}}\partial_{tj}\sigma = Q_j^- Q_j^+ - Q_j^+ Q_j^- = 0$. The angle measured from the fold set $\partial_{\mathbf{x}}\partial_{tj}\sigma = 0$ to the vector f^i is then denoted θ_j^i, where

$$\cos\theta_j^i = (f^i \cdot \varepsilon_j)/|f^i||\varepsilon_j|. \tag{51}$$

The angle between the folds is then the difference $\phi = \theta_+^+ - \theta_-^+ = \theta_+^- - \theta_-^-$, while the angle between f^+ and f^- is the difference $\psi = \theta_+^+ - \theta_+^- = \theta_-^+ - \theta_-^-$ (see figure 11).

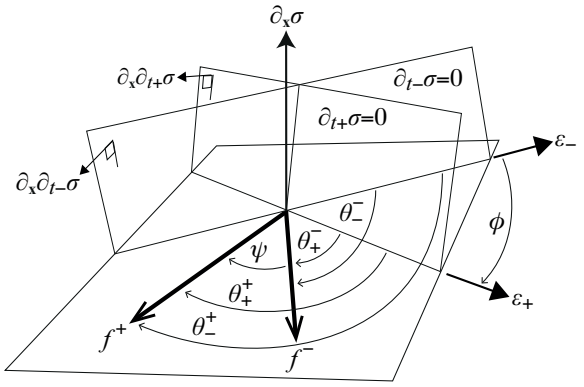

Figure 11: Local geometry behind the two-fold *angular jump* parameter v^+v^- as given by (54)-(55). The angle θ_j^i between the vector f^i and the fold $\partial_{tj}\sigma = 0$, the angle ϕ between the folds, and the angle ψ between f^+ and f^-. All angles are measured in the plane spanned by $f^{\pm}$, which lies inside (and in three dimensions is exactly) the tangent plane to the discontinuity surface $\sigma = 0$.

We can now find the required quantities Q_j^i in terms of the angles θ_j^i. First, calculate

$$\frac{\cos\theta_j^+}{\cos\theta_j^-} = \frac{(f^+ \cdot \varepsilon_j)/|f^+||\varepsilon_j|}{(f^- \cdot \varepsilon_j)/|f^-||\varepsilon_j|} = \frac{Q_j^-|f^+|^2 - Q_j^+ f^+ \cdot f^-}{Q_j^- f^- \cdot f^+ - Q_j^+|f^-|^2} \cdot \frac{|f^-|}{|f^+|}$$

which, substituting $f^+ \cdot f^- = |f^+||f^-|\cos\psi$, rearranges to give

$$\frac{|f^+|Q_j^-}{|f^-|Q_j^+} = \frac{\cos\psi\cos\theta_j^- - \cos\theta_j^+}{\cos\theta_j^- - \cos\psi\cos\theta_j^+}.$$

Using the relations $\psi = \theta_+^+ - \theta_+^- = \theta_-^+ - \theta_-^-$ we substitute

$$\frac{|f^+|Q_j^-}{|f^-|Q_j^+} = \frac{\cos\psi\cos\theta_j^- - \cos(\psi+\theta_j^-)}{\cos(\psi-\theta_j^+) - \cos\psi\cos\theta_j^+} = \frac{\sin\theta_j^-}{\sin\theta_j^+} \,.$$

Thus

$$\frac{Q_+^-Q_-^+}{Q_+^+Q_-^-} = \frac{\sin\theta_+^-}{\sin\theta_+^+}\frac{\sin\theta_-^+}{\sin\theta_-^-} \,.$$

Using the relations $\phi = \theta_+^+ - \theta_-^+ = \theta_+^- - \theta_-^-$ we substitute

$$\frac{Q_+^-Q_-^+}{Q_+^+Q_-^-} = \frac{\sin\theta_+^-\sin(\theta_+^+ - \phi)}{\sin\theta_+^+\sin(\theta_+^- - \phi)} = \frac{\cot\phi - \cot\theta_+^+}{\cot\phi - \cot\theta_+^-} \tag{52}$$

or

$$\frac{Q_+^-Q_-^+}{Q_+^+Q_-^-} = \frac{\sin(\theta_-^- + \phi)\sin\theta_-^+}{\sin(\theta_-^+ + \phi)\sin\theta_-^-} = \frac{\cot\phi + \cot\theta_-^-}{\cot\phi + \cot\theta_-^+} \,. \tag{53}$$

Finally then, from (49), measuring angles from to the '+' fold we have

$$v^+v^- = \alpha\frac{\cot\phi - \cot\theta_+^+}{\cot\phi - \cot\theta_+^-} \tag{54}$$

and measuring angles from to the '−' fold we have

$$v^+v^- = \alpha\frac{\cot\phi + \cot\theta_-^-}{\cot\phi + \cot\theta_-^+} \,. \tag{55}$$

The term α is just $-\mathrm{sgn}[(\partial_{t^+}^2\sigma)(\partial_{t^-}^2\sigma)]$, which is $+1$ if both folds are visible (section 5.1) or both are invisible (section 5.3), and is -1 if they are mixed (section 5.2). The term ϕ is the angle between the folds, and θ_j^i is the angle of f^i from the 'j' fold, measured in the plane spanned by f^+ and f^-.

B Piecewise smooth time rescaling

It is a simple but useful observation that the pattern of trajectories of a smooth system, called its *phase portrait*, remains unchanged if we rescale time by a strictly positive function. This remains true if the time scaling is piecewise-smooth. For completeness, let us show that applying different, strictly positive, time rescalings either side of the discontinuity surface, does not alter the phase portrait at the discontinuity surface itself.

We make a piecewise-smooth time rescaling $t \mapsto t/\mu(\mathbf{x})$, where

$$\mu(\mathbf{x}) = \begin{cases} \mu^+(\mathbf{x}) & \text{if} \quad \sigma(\mathbf{x}) > 0, \\ \mu^-(\mathbf{x}) & \text{if} \quad \sigma(\mathbf{x}) < 0, \end{cases} \tag{56}$$

with $\mu^{\pm}(\mathbf{x})$ strictly positive. The time scaling (56) does not change the phase portrait of the individual subsystems in $\sigma(\mathbf{x}) > 0$ or $\sigma(\mathbf{x}) < 0$, since they are smooth in those regions, so the only possible change in phase portrait would be on $\sigma(\mathbf{x}) = 0$. Firstly, the condition $(\partial_{t^+}\sigma)(\partial_{t^-}\sigma) > 0$ for transversality between the convex set $\frac{d}{dt}\mathbf{x}$ and the discontinuity is unchanged by the transformation, which multiplies the lefthand side by $\mu^+\mu^- > 0$, therefore crossing regions are preserved. When $(\partial_{t^+}\sigma)(\partial_{t^-}\sigma) < 0$ the flow's intersection with $\sigma = 0$ is characterised by the sliding flow with time derivative ∂_{t^s}. Substituting $t \mapsto t/\mu$ into (5), the Lie derivative transforms as $\partial_{t^s} \mapsto \mu'\partial_{t^s}$ where

$$\mu' = \frac{\mu^+\mu^-(\partial_{t^-} - \partial_{t^+})\sigma}{(\mu^-\partial_{t^-} - \mu^+\partial_{t^+})\sigma} = \frac{\mu^+\mu^-(|\partial_{t^-}\sigma| + |\partial_{t^+}\sigma|)}{|\mu^-\partial_{t^-}\sigma| + |\mu^+\partial_{t^+}\sigma|} > 0.$$

The second equality follows because $\partial_{t^+}\sigma$ and $\partial_{t^-}\sigma$ have opposite signs. Thus (56) scales time in the sliding flow by a strictly positive constant μ', so the transformation $t \mapsto t/\mu$ preserves the phase portrait of the flow.

References

[1] M. A. Aizerman and F. R. Gantmakher. On the stability of equilibrium positions in discontinuous systems. *Journal of Applied Mathematics and Mechanics (translated from the Russian Ob ustoichivosti polozhenii ravnovesiia v razryvnykh sistemakh)*, 24:283–93, 1960.

[2] E. Benoît, J. L. Callot, F. Diener, and M. Diener. Chasse au canard. *Collect. Math.*, 31-32:37–119, 1981.

[3] A. Colombo, M. di Bernardo, E. Fossas, and M. R. Jeffrey. Teixeira singularities in 3D switched feedback control systems. *Systems & Control Letters*, 59(10):615–622, 2010.

[4] A. Colombo, M. di Bernardo, S. J. Hogan, and M. R. Jeffrey. Bifurcations of piecewise smooth flows: perspectives, methodologies and open problems. *Physica D: Special Issue*, 241(22):1845–1860, 2012.

[5] A. Colombo and U. Galvanetto. Stable manifolds of saddles in piecewise smooth systems. *CMES*, 53:235–254, 2009.

[6] A. Colombo and U. Galvanetto. On the boundaries of basins of attraction in piecewise smooth systems. *Complexity in Engineering*, pages 100–102, 2010.

[7] A. Colombo and M. R. Jeffrey. Non-deterministic chaos, and the two-fold singularity in piecewise smooth flows. *SIAM J. App. Dyn. Sys.*, 10:423–451, 2011.

[8] M. Desroches and M. R. Jeffrey. Canards and curvature: nonsmooth approximation by pinching. *Nonlinearity*, 24:1655–1682, 2011.

[9] M. di Bernardo, C. J. Budd, A. R. Champneys, and P. Kowalczyk. *Piecewise-Smooth Dynamical Systems: Theory and Applications*. Springer, 2008.

[10] M. di Bernardo, A. Colombo, and E. Fossas. Two-fold singularity in nonsmooth electrical systems. *ISCAS*, pages 2713–2716, 2011.

[11] M. di Bernardo, P. Kowalczyk, and A. Nordmark. Bifurcations of dynamical systems with sliding: derivation of normal-form mappings. *Physica D*, 170:175–205, 2002.

[12] S. Fernández-García, D. Angulo-García, G. Olivar-Tost, M. di Bernardo, and M. R. Jeffrey. Structural stability of the two-fold singularity. *SIAM J. App. Dyn. Sys.*, 11(4):1215–1230, 2012.

[13] A. F. Filippov. *Differential Equations with Discontinuous Righthand Sides*. Kluwer Academic Publ. Dortrecht, 1988.

[14] M. R. Jeffrey. Non-determinism in the limit of nonsmooth dynamics. *Physical Review Letters*, 106(254103):1–4, 2011.

[15] M. R. Jeffrey and A. Colombo. The two-fold singularity of discontinuous vector fields. *SIAM Journal on Applied Dynamical Systems*, 8(2):624–640, 2009.

[16] M. R. Jeffrey and S. J. Hogan. The geometry of generic sliding bifurcations. *SIAM Review*, 53(3):505–525, 2011.

[17] Yu. A. Kuznetsov, S. Rinaldi, and A. Gragnani. One-parameter bifurcations in planar Filippov systems. *Int.J.Bif.Chaos*, 13:2157–2188, 2003.

[18] Yu. I. Neimark and S. D. Kinyapin. On the equilibrium state on a surface of discontinuity. *Radiophysics and Quantum Electronics (translated from the Russian Izvestiia vysshikh uchebnykh zavedenii. Radiofizika.)*, 3:694–705, 1960.

[19] M. A. Teixeira. Stability conditions for discontinuous vector fields. *J. Differ. Equ.*, 88:15–29, 1990.

[20] M. A. Teixeira. Generic bifurcation of sliding vector fields. *J.Math.Anal.Appl.*, 176:436–457, 1993.

[21] Various. Special issue on dynamics and bifurcations of nonsmooth systems. *Physica D*, 241(22):1825–2082, 2012.